THERMODYNAMICS OF FLOWS OF A POLYMERIZING, NONLINEARLY VISCOPLASTIC FLUID HAVING A FREE SURFACE

K. A. Chekhonin and V. K. Bulgakov

UDC 532.135

The finite elements method is used as a basis for proposing a numerical algorithm for the solution of the problem of the flow of a polymerizing viscoplastic fluid with a free surface. The effect of the main parameters of the problem on the character of the hydrodynamic process is explained.

The theoretical study of the hydrodynamics of flows of polymerizing, anomalously viscous fluids with a free surface is of practical importance for several areas of chemical and power engineering. Such flows are widely encountered in practical applications, such as in the formation of products of polymeric materials by injection molding.

Many investigators have been occupied with various aspects of the numerical study of flows of anomalously viscous fluids with a free surface in cylindrical channels. However, the results obtained in the well-known studies [1, 2] are applicable mainly to the investigation of nonreactive media. The authors of [3, 4] undertook a fairly detailed study of the flow of anomalously viscous media under nonisothermal conditions.

In the present investigation, we will examine the slow flow (Re < 1) of a polymerizing, nonlinearly viscoplastic fluid in the region between vertical coaxial cylinders. The theoretical flow region Ω_t, changing over time, is shown in Fig. 1a. We will assume that the density and thermophysical properties of the liquid are constant. The fluid flows under nonisothermal conditions in the presence of heat exchange with the environment through the wall of the outer cylinder. Also, heat is released due to dissipation of the energy of motion and the occurrence of the polymerization reaction. We will use the law generalized by Shul'man [5] for copper to describe the rheological behavior of the fluid:

$$\tau_{ij} = B(\nabla_i v_j + \nabla_j v_i), \quad i = j = 1;\ 3. \tag{1}$$

Here

$$B = \left[\frac{\tau_0^{1/n}}{A^{1/m}} + \mu_p^{1/m}\right]^n A^{\frac{n}{m}-1} \tag{2}$$

for a non-Newtonian fluid.

Given the initial premises, we see that the mathematical formulation of the problem will include the following equations:

the equation of continuity

$$\nabla_i v^i = 0, \quad i = 1;\ 3, \tag{3}$$

the equation of motion

$$\mathrm{Re}\left[\frac{\partial v^i}{\partial t} + \nabla_j (v^j v^i)\right] = \nabla_j \mu (\nabla_j v^i + \nabla_i v^j) - \nabla_i P - W_i, \tag{4}$$

the energy equation

$$\mathrm{Pe}\left[\frac{\partial \Theta}{\partial t} + \nabla_j (v^j \Theta)\right] = \Delta\Theta + \mathrm{Br}\,\mu A^2 + \mathrm{Bw}\left(\varkappa \frac{s\Theta}{1+s\Theta}\right)(1 - \beta_0 - \beta_* \beta)^\alpha, \tag{5}$$

Khabarovsk Polytechnic Institute. Translated from Inzhenerno-Fizicheskii Zhurnal, Vol. 59, No. 5, pp. 764-771, November, 1990. Original article submitted October 13, 1989.

0022-0841/90/5905-1395$12.50

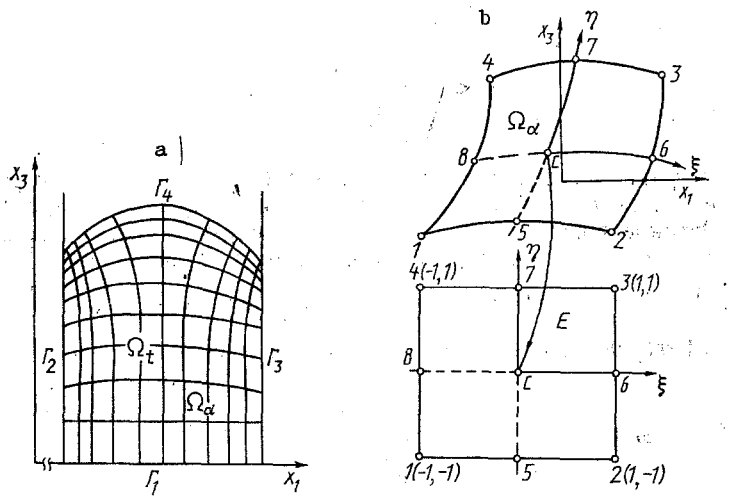

Fig. 1. Geometry and boundaries of the theoretical region (a) and a tetragonal isoperimetric element of second-order accuracy Ω_α (b); E) mapping of Ω_α in the local coordinate system η, ξ.

and the equation describing the macrokinetics of the polymerization reaction

$$\frac{\partial \beta}{\partial t} + \nabla_j (v^j \beta) = \mathrm{Ch}\left(\varkappa \frac{s\Theta}{1+s\Theta}\right)(1-\beta_0-\beta_*\beta)^\alpha. \tag{6}$$

The dependence of the rheological properties of the fluid on temperature and the degree of polymerization will be considered by means of the following relations:

$$\varphi_i = \varphi_i(\Theta_0, \beta_0)\exp[\tilde{\mathrm{Pn}}_i \beta - \mathrm{Pn}_i \Theta],$$
$$\varphi_1 = \mu_p, \quad \varphi_2 = \tau_0, \quad n = \mathrm{const}, \quad m = \mathrm{const}. \tag{7}$$

We will use the following as the boundary conditions of problem (3-7):

a) at the inlet Γ_1 of the flow region Ω_t (Fig. 1a), we assign the velocity profile of the steady-state flow with rheology (1); for the temperature and degree of polymerization, we adopt the initial conditions

$$\Theta(\mathbf{x})|_{\mathbf{x}\in\Gamma_1} = \Theta_0, \quad \beta(\mathbf{x})|_{\mathbf{x}\in\Gamma_1} = \beta_0; \tag{8}$$

b) on the solid walls Γ_2 and Γ_3 of the theoretical region Ω_t we have

$$\mathbf{V}|_{\mathbf{x}\in\Gamma_2,\Gamma_3} = V_0,$$
$$\left.\frac{\partial\Theta}{\partial \mathbf{n}}\right|_{\mathbf{x}\in\Gamma_2} = 0, \tag{9}$$
$$\left.\frac{\partial\Theta}{\partial \mathbf{n}}\right|_{\mathbf{x}\in\Gamma_3} = \mathrm{Bi}(\Theta_\infty - \Theta).$$

The last condition in (9) is adopted on the basis of the proposition $\Delta x_1/L \ll 1$ at $\lambda_{wa} \approx \lambda_q$.

On the free surface, we require satisfaction of the kinematic and dynamic conditions:

$$\frac{\partial \eta}{\partial t} + \mathbf{V}\cdot\nabla\eta = 0, \tag{10}$$

$$\{-P\delta_{ij} + \mu(\nabla_i v^j + \nabla_j v^i)\}\, n_j|_{\Gamma_4} = \hat{t}_j, \tag{11}$$
$$\hat{t}_1 = 0, \quad \hat{t}_3 = -P_0, \quad i, j = 1; 3.$$

For energy equation (5) we formulate the adiabatic condition

$$\left.\frac{\partial\Theta}{\partial \mathbf{n}}\right|_{\Gamma_4} = 0. \tag{12}$$

Thus, the problem of the flow of a polymerizing viscoplastic fluid with a free surface filling a prescribed region Ω amounts to the determination of Ω_t over time and the components of the velocity vector, pressure, temperature, and non-Newtonian viscosity that satisfy Eqs. (3-12).

When system (3-12) is solved, the continuity equation is customarily replaced by the Poisson equation for pressure [2]. This equation has a complicated form and is characterized by weak convergence during numerical solution.

Here, we will make use of an algorithm that was proposed in [6]. He will represent the sought velocity and pressure fields in the form of sums of the approximate values ($\tilde{v}$, $\tilde{P}$) and corrections (v', P')

$$v_i = \tilde{v}_i + v_i', \quad P = \tilde{P} + P', \quad i = 1; 3. \tag{13}$$

To determine v' and P', we will use the Prakht velocity-correction potential Ψ [6, 14]. Here,

$$v_i' = \frac{d\Psi}{dx_i}, \quad P' = -\frac{2\rho}{\Delta t}\Psi. \tag{14}$$

The distribution of the potential Ψ in the flow region Ω_t will be found from the Poisson equation

$$\Delta\Psi = -\operatorname{div}\mathbf{V} \tag{15}$$

with homogeneous Neumann boundary conditions

$$\left.\frac{\partial\Psi}{\partial n_\alpha}\right|_{\Gamma_\alpha} = 0, \quad \alpha = \overline{1, 4}. \tag{16}$$

The numerical solution of the problem is based on the finite-element method with the use of Galerkin's weighted errors [7]. The flow region Ω_t is subdivided into eight-node isoperimetric finite elements Ω_α (Fig. 1b) in such a way that $\Omega_t = \bigcup_\alpha \Omega_\alpha$. We construct the finite-element grid automatically in accordance with an algorithm [8] adapted to the solution of the problem. We approximate the main variables v_i, Θ, β and Ψ in the element Ω_α with the use of quadratic basis functions, while we approximate pressure by means of linear basis functions [9]:

$$v_i = \sum_{\alpha=1}^{8} N_\alpha v_\alpha^i, \quad \Psi = \sum_{\alpha=1}^{8} N_\alpha \Psi_\alpha, \quad \Theta = \sum_{\alpha=1}^{8} N_\alpha \Theta_\alpha,$$
$$\beta = \sum_{\alpha=1}^{8} N_\alpha \beta_\alpha, \quad P = \sum_{\alpha=1}^{4} F_\alpha P_\alpha. \tag{17}$$

After we insert Eqs. (17) into Eqs. (4-6), (13), and (15), integrate, and reduce the results to global form, we can represent them in the form of the following system of matrix equations:

$$[M]\{v_t^i\} + [G]\{v^i\} = \{F_1\}, \tag{18}$$
$$[S]\{\Psi\} = \{F_2\}, \tag{19}$$
$$[\overline{M}]\{v_t^i\} = [\overline{M}]\{\tilde{v}_t^i\} + [H^i]\{\Psi\}, \tag{20}$$
$$[C]\{\Theta_t\} + [T]\{\Theta\} = \{F_3\}, \tag{21}$$
$$[B]\{\beta_t\} + [K]\{\beta\} = \{F_4\}. \tag{22}$$

We solve system of nonlinear equations (18) iteratively with the use of the adaptive procedure of the SOR method [10]. Integration of Eqs. (21-22) over time is done in accordance with the Crank–Nicolson scheme. The equations are then solved by the frontal method [10].

Second- and third-order boundary conditions are accounted for automatically in projection-grid equations (18-22). The first-order boundary conditions are numerically realized in accordance with the Payne–Aarons algorithm [12]. As the initial conditions of the problem, we will use the fields of velocity, pressure, temperature, degree of polymerization, and effective viscosity obtained when the problem is solved with a plane free surface.

The algorithm used to solve the problem is conveniently broken down into two cycles: isothermal and nonisothermal. With allowance for this, we can represent the algorithm in the form of the following successive computing operations: a) in the first cycle, we use the projection-grid equations (18) to determine the approximate velocity field v_i for the (n + 1)-th iteration, with the value of non-Newtonian viscosity (μ) being taken from the n-th iteration; we use the resulting velocity field and (19) to determine the potential distribution and, thus, the corrections to velocity and pressure; we use (13) to find the corrected velocity and pressure fields; we continue the iteration until satisfaction of the convergence conditions

$$\max_i \|\Phi_i^{n+1} - \Phi_i^n\| < \max_i |\Phi_i^n| \varepsilon_i;$$

b) in the nonisothermal cycle, we use Eqs. (21) and (22) to find the fields of temperature and degree of polymerization; we use Eqs. (7) to correct the rheological parameters of the fluid as a function of temperature and degree of polymerization and, thus, the field of non-Newtonian viscosity μ; the isothermal cycle is then repeated. After convergence of the iterative process, we make a time step and we use kinematic condition (10) to determine the new position of the free surface. Its form is approximated by splines. We complete the finite-element grid in the resulting region $\Omega_{t+\Delta t}$ and again solve Eqs. (18-22). Thus, an acceptable solution to the problem will be satisfaction of the condition $\Psi = 0$ for all nodes of the grid, since in this case the values of v_i and P in (13) will be exact values of the components of the velocity vector and pressure, respectively. Proceeding on the basis of these considerations, the equation for Ψ (15) can be regarded as an intermediate algorithm which allows us to determine the exact fields of velocity and pressure without directly affecting the final solution of the problem. It should be noted that the above-examined iterative algorithm does not converge if lower relaxation is not used in the solution of Eqs. (18-19). This is evidently the result of the strong nonlinearity of the problem and the incompatibility of the gradient Ψ at the boundaries of the region Ω_t with the source term in the Poisson equation (15). Here,

$$\int_{\Omega} \nabla_i v^i d\Omega_\alpha = \int_{\partial\Gamma} \frac{\partial \Psi}{\partial x_i} n_i dS.$$

In the present study, we took $\omega_V = \omega_\Psi = 0.1$ for the initial relaxation factors. Using the adaptive procedure in [10], these factors were subsequently reduced to the values $\omega_V = 0.5$, $\omega_\Psi = 0.75$.

Another important feature of the numerical solution of the problem is manifest in studies of flows with a large Peclet number ($P_h > 2$). In this case, convective terms will play the deciding role in the energy equation. Thus, the diagonal elements of the thermal conductivity matrix will be unimportant and, given the boundary conditions we have assigned for the problem, its solution will be of an oscillating character. To avoid undesirable oscillations, we can use a finer grid [3] and satisfy the condition $P_h < 2$. However, this leads to a substantial increase in computing time. To eliminate the numerical instability in our problem, we approximated the energy equation by introducing asymmetric weight functions [13]. Such functions are the analog of differences against the flow in the finite-difference method.

The results of the calculation are conveniently analyzed with the use of dimensionless complexes: W, Gr_i, Lw_i, $\tilde{Gr}_i$, St. In this case, with a prescribed flow-region geometry and prescribed values for the coefficients n, m, and α, these complexes fully characterize the hydrodynamic process. The effect of the parameters W, Gr_i, St, n, m on the character of the hydrodynamic process was studied in [3, 4, 6].

In the present investigation, we will restrict ourselves to study of the effect of the parameters $\tilde{Gr}_i$ and Lw_i when the values of the constants n = 1.1, m = 1.3, α = 1. Figure 2 shows the evolution of the maximum deflection of the front of the free surface over time. Analysis of the results of the calculation shows that, for the isothermal case, the free surface is established beginning from a certain moment of time $t \approx L/UH$. This is also evidence of the establishment of the front of the free surface, which subsequently moves in the direction of the Ox_3 axis at a constant rate equal to the flow-rate-mean velocity of the flow at the inlet Γ_1. One characteristic hydrodynamic feature of the nonisothermal flow of a viscoplastic fluid which undergoes structuring over time is that the evolution of the surface does not occur at an established position. An increase in the parameters Lw_i

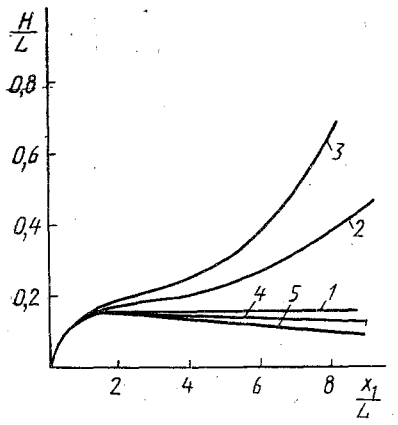

Fig. 2

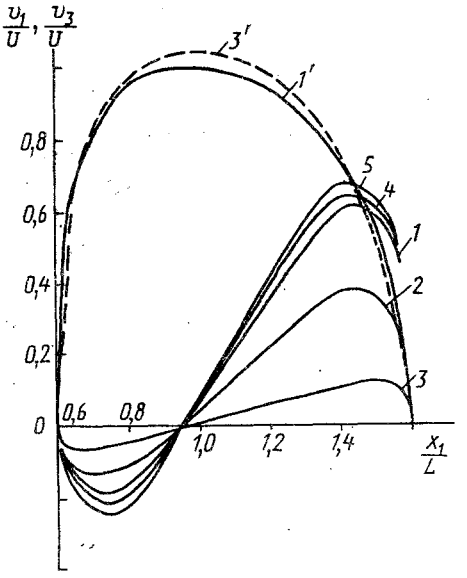

Fig. 3

Fig. 2. Evolution of the maximum deflection of the front of the free surface: 1 — isothermal case $W=53$; 2 — $W=53$; $Gr_1=3{,}6\cdot10^{-2}$, $Gr_2=2{,}9\cdot10^{-6}$, $\tilde{G}r_1=1{,}4\cdot10^{-3}$, $\tilde{G}r_2=1{,}7\cdot10^{-3}$, $Lw_1=4\cdot10^{-2}$, $Lw_2=7{,}1\cdot10^{-2}$, $St=0{,}81$; 3 — $Lw_1=9{,}4\cdot10^{-2}$, $Lw_2=0{,}111$; 4 — $Gr_1=1{,}4\cdot10^{-2}$, $Gr_2=1{,}7\cdot10^{-2}$; 5 — $\tilde{G}r_1=4{,}8\cdot10^{-2}$, $Gr_2=6{,}1\cdot10^{-2}$.

Fig. 3. Profile of radial (1-5) and axial (1', 3') components of the velocity vector on the free surface of the liquid at the moment of time t = 6 L/U at the parameter values shown in Fig. 2.

leads to an increase in the maximum convexity of the free surface and, thus, to a reduction in the intensity of the strain rates on it (Fig. 3).

The situation is different in regard to the study of flows in which the Griffith parameters have the determining effect. In this case, an increase in the parameters $\tilde{G}r_i$ leads to a decrease in the maximum deflection of the front over time. This reduction can be attributed directly to a decrease in effective viscosity in the region of the free surface and, thus, a reduction in strain-rate intensity on it. As a result, an increase in the parameters Lw_i leads to an increase in the adaptive properties of the fluid over time, while an increase in $\tilde{G}r_i$ leads to an increase in its pseudoplastic properties. It must also be noted that an increase in the parameters Lw_i leads to a substantial increase over time in the dimensions of the zone of intensive radial flow (D_R) in the vicinity of the free surface. Thus, examination of two variants for filling out the region Ω with the parameter values $Lw_i = 0$ and $Lw_i = 0.43$ led to doubling of the dimensions D_R at the moment of time t = 4. However, a change in the Griffith parameters within the range $1\cdot10^{-4} \leq \tilde{G}r_i \leq 1\cdot10^{-2}$ produced almost no change in the dimensions D_R.

It is interesting to consider the effect of the parameters Lw_i and $\tilde{G}r_i$ on the character of fluid distribution in the case of batch filling of the region Ω. We will introduce marker particles to visualize the flow pattern in the theoretical region Ω_t. Their position over time is determined from the kinematic condition

$$x_i^{n+1} = x_i^n + \hat{v}_i \Delta t.$$

We find the components of the velocity vector of the markers ($\hat{v}_i$) in finite element Ω_α from interpolation formulas (17). Figure 4 shows the effect of the parameters $\tilde{G}r_i$ and Lw_i on the character of the mass distribution of 10 batches of fluid. The batches fed into the region at time intervals $\Delta t = 0.3$ with values of the parameters $W = 8.1$, $Gr_1 = 3.6\cdot10^{-5}$, $Gr_2 = 4.1\cdot10^{-5}$, $\tilde{G}r_1 = 1.7\cdot10^{-3}$, $\tilde{G}r_2 = 6.4\cdot10^{-3}$, $Lw_1 = 0.1$, $Lw_2 = 0.25$, $St = 4\cdot10^{-3}$, $n = 0.8$, $m = 1.6$, $\alpha = 2$. For comparison, we simultaneously calculated the pattern of mass distribution under isothermal conditions for a nonreactive fluid. It follows from the results that allowing for changes in the structural properties of the fluid under nonisothermal condi-

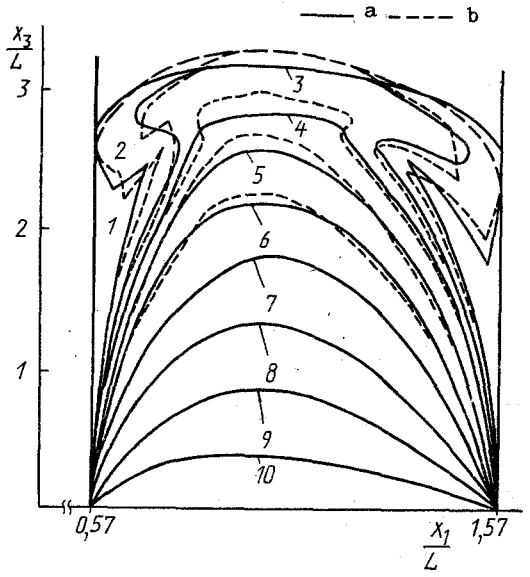

Fig. 4. Pattern of mass distribution of 10 batches of fluid: a) isothermal case with $Lw_i = 0$; b) with allowance for the change in the structural properties of the batches.

tions can have a significant effect on the character of the mass distribution. The effect of the above parameters on the mass distribution will be determined by the quantity $\delta_i = \tilde{G}r_i/Lw_i$, so that at $\delta_i \ll 1$ the determining effect will be exerted by structural changes in the fluid resulting from the polymerization reaction. At $\delta_i \gg 1$, the nonisothermal nature of the process will be decisive. The numerical calculations showed that, other conditions being equal, an increase in the parameters Lw_2 and Gr_2, such that $Lw_2 > 0.1$, $\tilde{G}r_2 > 0.1$ and $\delta_2 \gg 1$ or $\delta_2 \ll 1$, will produce the largest changes in mass distribution over time.

NOTATION

v^1, v^3, radial and axial components of velocity; $A = \sqrt{2e_{ij}e_{ji}}$, intensity of the strain rates; $e_{ij} = 0.5(\nabla_i v^j + \nabla_j v^i)$, strain-rate tensor; τ_{ij}, deviator of the stress tensor; τ_0, flow stress; μ_p, plastic viscosity; n, m, coefficients of the nonlinear rheological model; P, pressure: $\mu = B/\mu_e$, dimensionless coefficient of non-Newtonian viscosity; $\mu_e = [\tau_0^{1/n} + (\mu_p A_{av})^{1/m}]^n/A_{av}$, effective viscosity; $A_{av} = U/L$; U, flow-rate-mean velocity; $L = R_2 - R_1$; R_1, R_2, radii of the internal and external tubes; $\Theta = (T - T_0)/T_*$, dimensionless temperature; T, T_0, running and initial value of temperature; $T_* = (\mu, A_{av} + Q\beta_*)/\rho c$, characteristic temperature gradient; Q, amount of heat released during the polymerization reaction; β, degree of polymerization; β_*, characteristic change in the degree of polymerization during the filling of the region; $\kappa = E/RT_0$; E, activation energy of the reaction; $s = T_*/T_0$; α, order of the reaction; $Re = \rho UL/\mu_e$, Reynolds number; $W_3 = Re/Fr$; $Fr = U^2/Lg$, Froude number; $W_1 = 0$; $Pe = \rho CUL/\lambda$, Peclet number; $Br = \mu_e U^2/\lambda T_*$, Brinkman number; $Bw = QK_0L^2/(T_*\lambda \exp(\kappa))$; $Ch = K_0L(\beta_* U \exp(\kappa))^{-1}$; $Bi = hL/\lambda$, Biot number; h, heat-transfer coefficient; F_α, N_α, linear and quadratic basis functions; [M], "mass" matrix; [G], "stiffness" matrix; [C], "heat capacity" matrix; [K], "thermal conductivity" matrix; [B], "polymerization" matrix; [K], "convection" matrix; [S], "potential" matrix; $\{v^i\}$, $\{F_1\}$, vectors of the unknowns and the "loads"; $Ph = \rho U\Delta xC/\lambda$, grid Peclet number; Δx, maximum step of finite-element grid; $Gr_1 = Br\ Sn\ Pn_1$; $Gr_2 = Br\ Se\ Pn_2$; $\tilde{G}r_1 = Bw\ Se\ \tilde{P}n_1$, $\tilde{G}r_2 = Bw\ Sn\ Pn_2$, Griffith numbers; $\tilde{P}n_i = a_i\beta_*$, $Pn_i = b_iT_*$, Pearson numbers; a_i, b_i, constants of the medium; $Sn = \mu_p/\mu_e$, $Se = \tau_0/\mu_e A_{av}$; $Lw_1 = Ch\ Sn\ \tilde{P}n_1$; $Lw_2 = Ch\ Se\ Pn_2$; $St = Bi/Pe$, Stanton number; $\eta(x, t)$, equation of the free surface; λ, thermal conductivity of the fluid; ρ, density; C, heat capacity; Δ, Laplace operator; K_0, rate constant of reaction; g, acceleration due to gravity.

LITERATURE CITED

1. V. P. Ishchenko and A. N. Kozlobrodov, Izv. Sib. Otd. Akad. Nauk SSSR Ser. Tekh. Nauk, No. 5, 34-42 (1985).

2. V. K. Bulgakov, A. M. Lipanov, K. A. Chekhonin, and O. N. Ivanov, Mekhanika Kompozitnykh Materialov, No. 6, 1112-1116 (1988).
3. V. K. Bulgakov, K. A. Chekhonin, and I. A. Glushkov, Methods of Improving the Quality, Reliability, and Durability of Engineering Structures [in Russian], Khabarovsk (1988), pp. 25-30.
4. V. K. Bulgakov, A. M. Lipanov, and K. A. Chekhonin, Inzh.-Fiz. Zh., 57, No. 4, 577-583 (1989).
5. Z. P. Shul'man, Convective Heat and Mass Transfer of Non-Newtonian Fluids [in Russian], Moscow (1975).
6. V. K. Bulgakov and A. M. Lipanov, Models of the Mechanics of Inhomogeneous Systems [in Russian], Novosibirsk (1989), pp. 242-260.
7. J. Connor and K. Brebbia, The Finite-Element Method in Fluid Mechanics [Russian translation], Leningrad (1979).
8. K. A. Chekhonin, Modeling and Optimization of Production Processes [in Russian], Khabarovsk (1989), pp. 43-48.
9. K. A. Chekhonin, "Numerical modeling of flows of non-Newtonian fluids by the finite-element method," Submitted to VINITI, No. 2656–88 (1988).
10. L. Hageman and D. Yang, Applied Iteration Methods [Russian translation], Moscow (1986).
11. R. A. Walters, Comput. Fluids, 2, 265-272 (1980).
12. O. Zenkevich, The Finite-Element Method in Engineering [Russian translation], Moscow (1975).
13. K. Fletcher, Numerical Methods Based on the Galerkin Method [Russian translation], Moscow (1988).
14. W. Prakht, Numerical Methods and Fluid Mechanics, Moscow (1973), pp. 174-182.

EXPERIMENTAL STUDY OF HEAT TRANSFER IN LIQUID-NITROGEN COOLING OF THE SURFACE OF SUPERCONDUCTING $YBa_2Cu_3O_7$ CERAMIC. 2. BURNOUT IN NUCLEATE BOILING

V. V. Baranets, Yu. A. Kirichenko,
S. M. Kozlov, S. V. Nozdrin,
K. V. Rusanov, and E. G. Tyurina

UDC 536.248.2.001.5

Burnout in the nucleate boiling of nitrogen on flat horizontal metal-oxide ceramic heaters is investigated in the pressure range from $1.3 \cdot 10^4$ Pa to $4.5 \cdot 10^5$ Pa.

We have previously [1] investigated the characteristics of heat transfer in the nucleate boiling of nitrogen on ceramic samples at low to moderate heat flux densities q. Here we give the results of a study of heat transfer at heat inputs approaching burnout, along with the characteristics of nucleate boiling burnout. The first critical (first-stage burnout) heat flux density q_{cr1} and the corresponding differential temperature ΔT_{cr1} are important parameters in calculating the stabilization conditions for current-carrying superconductors cooled by a boiling cryogen [2]. The literature to date does not contain any data on q_{cr1} and ΔT_{cr1} for the boiling of nitrogen on high-temperature superconducting (HTSC) materials. Because of the porous structure and low thermal conductivity λ_N of ceramics [3], these two critical quantities can be assumed to differ from the typical values for boiling on metal surfaces.

The experiments were carried out in a metal cryostat on samples of the superconducting yttrium ceramic $YBa_2Cu_3O_7$ with thicknesses of 3.1 mm and 2.0 mm (samples No. 2 and No. 4 in

Physicotechnical Institute of Low Temperatures, Academy of Sciences of the Ukrainian SSR, Kharkov. Translated from Inzhenerno-Fizicheskii Zhurnal, Vol. 59, No. 5, pp. 772-775, November, 1990. Original article submitted September 5, 1989.

